Neural Networks 43 (2013) 114–124

Contents lists available at SciVerse ScienceDirect

Neural Networks

journal homepage: www.elsevier.com/locate/neunet

A common framework of signal processing in the induction of cerebellar LTD and cortical STDP

Minoru Honda [a,1,2], Hidetoshi Urakubo [b,1,3], Takuya Koumura [c,4], Shinya Kuroda [a,b,c,*]

[a] Department of Computational Biology, Graduate School of Frontier Sciences, University of Tokyo, 5-1-5 Kashiwanoha, Kashiwa 277-8561, Japan
[b] Department of Biophysics and Biochemistry, Graduate School of Science, University of Tokyo, Hongo 7-3-1, Bunkyo-ku, Tokyo 113-0033, Japan
[c] Department of Bioinformatics and Systems Biology, School of Science, University of Tokyo, Hongo 7-3-1, Bunkyo-ku, Tokyo 113-0033, Japan

ARTICLE INFO

Article history:
Received 29 February 2012
Received in revised form 21 January 2013
Accepted 26 January 2013

Keywords:
Cerebellar LTD
Cortical STDP
Signaling pathways
System model

ABSTRACT

Cerebellar long-term depression (LTD) and cortical spike-timing-dependent synaptic plasticity (STDP) are two well-known and well-characterized types of synaptic plasticity. Induction of both types of synaptic plasticity depends on the spike timing, pairing frequency, and pairing numbers of two different sources of spiking. This implies that the induction of synaptic plasticity may share common frameworks in terms of signal processing regardless of the different signaling pathways involved in the two types of synaptic plasticity. Here we propose that both types share common frameworks of signal processing for spike-timing, pairing-frequency, and pairing-numbers detection. We developed system models of both types of synaptic plasticity and analyzed signal processing in the induction of synaptic plasticity. We found that both systems have upstream subsystems for spike-timing detection and downstream subsystems for pairing-frequency and pairing-numbers detection. The upstream systems used multiplication of signals from the feedback filters and nonlinear functions for spike-timing detection. The downstream subsystems used temporal filters with longer time constants for pairing-frequency detection and nonlinear switch-like functions for pairing-numbers detection, indicating that the downstream subsystems serve as a leaky integrate-and-fire system. Thus, our findings suggest that a common conceptual framework for the induction of synaptic plasticity exists despite the differences in molecular species and pathways.

1. Introduction

Synaptic plasticity is thought to be a molecular and cellular basis of our learning and memory. Cerebellar long-term depression (LTD) (Ito, 1989) and cortical spike-timing-dependent synaptic plasticity (STDP) (Caporale & Dan, 2008; Sjostrom, Rancz, Roth, & Hausser, 2008; Urakubo, Honda, Tanaka, & Kuroda, 2009) are two well-known and well-characterized types of synaptic plasticity. Cerebellar LTD is thought to be a molecular and cellular basis for cerebellar motor learning (Doya, 2000; Ito, 1989; Kawato, 1999; Kawato, Kuroda, & Schweighofer, 2011; Lisberger, 1998; Tsuruno & Hirano, 2011). Cerebellar LTD is a process involving a long-term decrease in the synaptic strength between parallel fiber (PF) and Purkinje cells (PC) induced by repetitive pairing stimulation of PF and climbing fiber (CF) (Ito, 1989; Linden & Connor, 1995). STDP has been shown to play an important role in neural development and information processing in the brain (Caporale & Dan, 2008; Sjostrom et al., 2008; Urakubo et al., 2009), such as the acquisition of orientation and direction selectivity in the primary visual system (Engert, Tao, Zhang, & Poo, 2002; Honda, Urakubo, Tanaka, & Kuroda, 2011; Schuett, Bonhoeffer, & Hubener, 2001; Yao & Dan, 2001). STDP is a process involving a long-term increase in synaptic strength (i.e., long-term potentiation, LTP) and a long-term decrease in synaptic strength, LTD, depending on the timing between pre- and postsynaptic spiking (pre-spiking and post-spiking, respectively) (Caporale & Dan, 2008; Sjostrom et al., 2008; Urakubo et al., 2009). Induction of STDP also requires the repetitive pairing stimulation of pre- and post-spiking. The signaling pathways that regulate the induction of both types of synaptic plasticity are different and complex (Bhalla & Iyengar, 1999; Caporale & Dan, 2008; Ito, 1989; Urakubo et al., 2009; Weng, Bhalla, & Iyengar, 1999); however, they share some similar signal processing. The signals pairing of two different types

* Corresponding author at: Department of Biophysics and Biochemistry, Graduate School of Science, University of Tokyo, Hongo 7-3-1, Bunkyo-ku, Tokyo 113-0033, Japan. Tel.: +81 3 5841 4697; fax: +81 3 5841 4698.
E-mail address: skuroda@bi.s.u-tokyo.ac.jp (S. Kuroda).

[1] These authors contributed equally to this work.

[2] Present address: Research and Development Laboratory, Nihon Kohden Corporation, Nishiochiai 1-31-4, Shinjuku-ku, Tokyo, 161-8560, Japan.

[3] Present address: Department of Systems Science, Graduate School of Informatics, Kyoto University, Uji 611-0011, Japan.

[4] Present address: Department of Life Sciences, Graduate School of Arts and Sciences, University of Tokyo, Komaba 3-8-1, Meguro-ku, Tokyo 153-8902, Japan.

0893-6080/$ – see front matter © 2013 Elsevier Ltd. All rights reserved.
doi:10.1016/j.neunet.2013.01.018

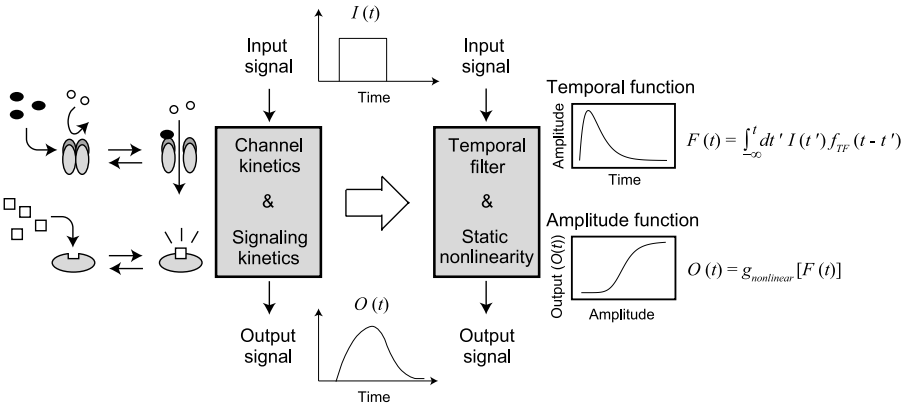

Fig. 1. Description of biophysical and biochemical reaction kinetics using temporal filters and static nonlinear functions. In the kinetic models, an input signal, $I(t)$, was transduced through channel kinetics and signaling kinetics to produce an output signal, $O(t)$. If a ligand (black ellipse) binds to a receptor (gray ellipse), this leads to channel opening, which conducts small ions (white circle). Also, a molecular–molecular interaction (white square and gray ellipse) contributes to signal transduction by the mechanism of allosteric kinetics. In contrast, in the system models, an input signal, $I(t)$, passed through temporal filters, $F(t)$, with kernel functions, $f_{TF}(t)$, and static nonlinear functions, $g_{nonlinear}[F(t)]$, and was converted to an output signal $O(t)$.

of spiking are encoded into temporal patterns of Ca^{2+}, which are further decoded by the downstream signaling pathways to regulate long-lasting plastic changes in synaptic strength (Caporale & Dan, 2008; Ito, 1989; Sjostrom et al., 2008; Urakubo et al., 2009). To understand the mechanisms underlying the induction of both types of synaptic plasticity, detailed kinetic models of cerebellar LTD (Brown, Morgan, Watras, & Loew, 2008; Doi, Kuroda, Michikawa, & Kawato, 2005; Hernjak et al., 2005; Kotaleski, Lester, & Blackwell, 2002; Kuroda, Schweighofer, & Kawato, 2001) and cortical STDP (Honda et al., 2011; Karmarkar & Buonomano, 2002; Rubin, Gerkin, Bi, & Chow, 2005; Shouval, Bear, & Cooper, 2002; Urakubo, Honda, Froemke, & Kuroda, 2008) have been developed. Although these kinetic models are powerful tools for providing molecular mechanistic insights, it is intuitively difficult to capture the essential frameworks because of the complex nature of the signaling pathways. On the other hand, the function of signaling pathways can be regarded as signal processing (Alon, 2007; Waltermann & Klipp, 2011). Therefore, we characterized the signaling pathways as signal processing by using temporal filters and static nonlinear functions that are able to capture the behaviors of the signaling process in time and amplitude, respectively.

To explicitly extract the essential frameworks of the complex signaling pathways, we reduced the detailed kinetic models of cerebellar LTD and cortical STDP by employing temporal filters and static nonlinear functions (Hill equation) (Endeman & Kamermans, 2010) and developed system models of the signaling pathways in the induction of both types of synaptic plasticity. Both models were able to capture the essential characteristics of the induction of synaptic plasticity. The system models revealed that both types of synaptic plasticity share a common framework, with tandem subsystems for spike-timing detection, and for pairing-frequency and pairing-numbers detection. The upstream subsystem uses multiplication of signals from feedback filters and nonlinear functions for spike-timing detection. The downstream subsystems use a temporal filter with longer time constants and nonlinear switch-like functions, which serve as a leaky integrate-and-fire system of upstream signals, for the pairing-frequency and pairing-numbers detection, respectively.

2. Results

2.1. A system model by using temporal filters and static nonlinear functions

The elementary process underlying signal processing in the induction of synaptic plasticity is the kinetics of ion channels and biochemical reactions. To illustrate the kinetics more explicitly in time and amplitude, we constructed computational models of synaptic plasticity using temporal filters and static nonlinear functions (Fig. 1, Appendix A). Temporal filters capture time-varying characteristics in the dynamic relationship between input and output signals, which explicitly characterize the time scale of a reaction. A static nonlinear function transforms the instantaneous amplitude of an input signal to that of an output signal, which explicitly characterizes the dose–response of a reaction. A Hill equation, a steady-state solution of a biochemical reaction, was used for most static nonlinear functions. Here, we tried to give a reduced description of a linear cascade of signaling pathways by a set of a temporal filter and static nonlinear function. This reduction of biophysical and biochemical models makes it easier to understand signal processing and analysis of the system dynamics.

In this study, we focused on two well-known types of long-term synaptic plasticity, cerebellar LTD and cortical STDP, whose detailed signaling pathways have been previously modeled using kinetic differential equations (Brown et al., 2008; Doi et al., 2005; Hernjak et al., 2005; Karmarkar & Buonomano, 2002; Kotaleski et al., 2002; Kuroda et al., 2001; Rubin et al., 2005; Shouval et al., 2002; Urakubo et al., 2008). From the kinetic models, we extracted the signaling pathways minimally necessary for reproduction of major characteristics of cerebellar LTD and cortical STDP, and each linear cascade of the pathways was described by a set of a temporal filter and static nonlinear function. The reduced models are denoted as system models of cerebellar LTD and cortical STDP. Signal processing in the induction of both types of synaptic plasticity has similar traits: spike-timing signals are encoded into temporal patterns of Ca^{2+}, which are further decoded by the downstream signaling pathways to regulate long-lasting plastic changes in synaptic weights. In this study, we developed and analyzed the system models of cerebellar LTD (see Figs. 2 and 3) and of cortical STDP (see Figs. 4 and 5) and extracted essential frameworks of both types of synaptic plasticity (Fig. 6).

Note in the reduction process, the temporal patterns of Ca^{2+} were normalized as the integrated Ca^{2+} by a single CF or post-spike became 1, and the unit of Ca^{2+} was dimensionless. The concentrations of downstream molecules were also normalized by maximal concentration of active molecules (max = 1). Accordingly, the dissociation constants (*Kds*) represent the relative sensitivities of downstream molecules to upstream molecules, and their units are also dimensionless (Tables 1 and 2). Only time has a unit (msec) in the present study.

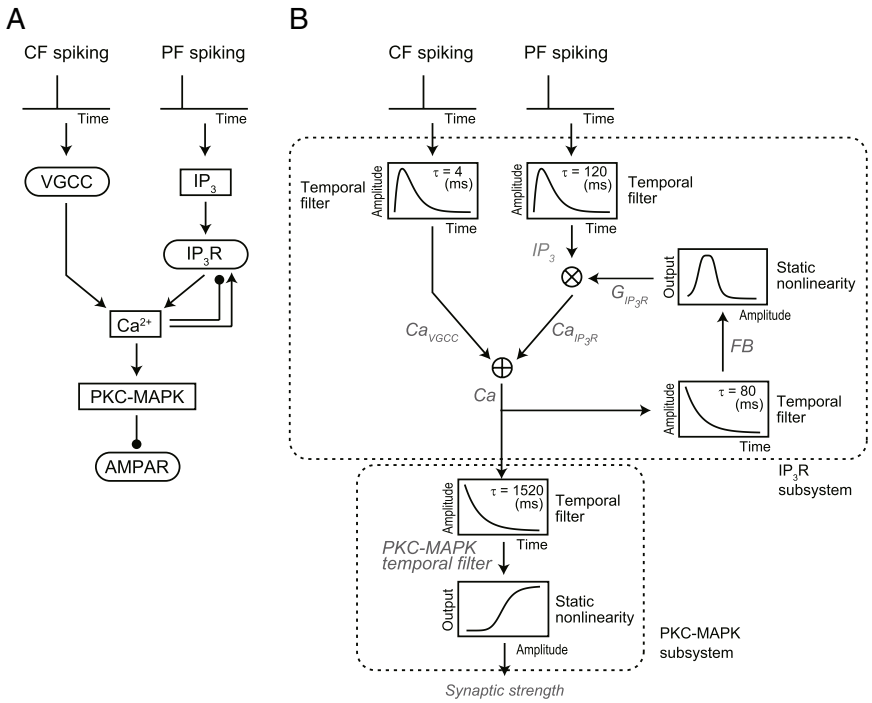

Fig. 2. The kinetic and system models of cerebellar LTD. Input signals (PF spiking and CF spiking) were converted to the changes of synaptic strength. (A) The kinetic model of cerebellar LTD. The squares enclose names of intracellular molecules, and the rounded squares enclose names of channels or receptors. The arrows depict the relations between upstream and downstream, with sharp point meaning activation and a circle meaning suppression. (B) The system model of cerebellar LTD, which consists of temporal filters and static nonlinear functions. The arrows depict the information flows. Gray and italic words indicate the names of signals (variables). Curves in the square boxes depict shapes of the filters and functions. τ represents the time constant of each temporal filter. The dashed boxes enclose the IP_3R and PKC–MAPK subsystems.

Table 1
Parameters of the cerebellar LTD model.

Name	Value	Reference
τ_{PF}	120 ms	(Doi et al., 2005; Okubo et al., 2004)[b]
τ_{FB}	80 ms	(Doi et al., 2005)[b]
k	1.04	(Bezprozvanny et al., 1991)[a,b]
K	1.04	(Bezprozvanny et al., 1991)[a,b]
n_{IP_3R}	2.7	(Bezprozvanny et al., 1991)[b]
Amp_{IP_3R}	7750	[a]
τ_{CF}	10 ms	(Doi et al., 2005)[b]
Ca_{basal}	0.0416	[a]
τ_{ST}	1520 ms	(Tanaka et al., 2007)
Kd_{ST}	8	[a]
n_{ST}	0.34	
Amp_{ST}	35%	(Ito, 1989; Tanaka et al., 2007)[a]

[a] Molecular concentrations, dissociation constants, and amplification factors are dimensionless.
[b] The parameters were estimated accordingly to reproduce the behavior in the detailed model (Doi et al., 2005). Note that parameters in the reduced model do not directly correspond to those in experiments nor to biophysical parameters in the detailed model because parameters in the reduced model can be regarded as compressed parameters of several reactions.

2.2. System model of cerebellar LTD

To extract the essential framework of the signaling pathway in the induction of cerebellar LTD, we reduced the detailed kinetic model of cerebellar LTD (Fig. 2(A), Appendix B) (Doi et al., 2005; Kuroda et al., 2001) and developed a system model of cerebellar LTD by using temporal filters and static nonlinear functions (Hill equations). This model has eight variables, which describe the representative signaling activities (Fig. 2(B), gray and italic words). Repetitive pairing of a PF-spike burst followed by a CF spike, but neither the opposite spike timing nor PF or CF spiking alone, induced large Ca^{2+} (Ca) (Doi et al., 2005; Wang, Denk, & Hausser, 2000) and consequently reduced synaptic strength (i.e., LTD; Fig. 3(A)–(C)) (Safo & Regehr, 2008).

Table 2
Parameters of the cortical STDP model.

Name	Value	Reference
Amp_{NMDAR}	1.36	[a]
τ_{NMDAR}	12 ms	(Feldmeyer et al., 2002)[b]
τ_{BAP}	4 ms	(Sabatini et al., 2002)[b]
τ_{FB}	10 ms	(Urakubo et al., 2008)[c]
κ	0.0114	(Urakubo et al., 2008)[c]
n_{FB}	1	(Urakubo et al., 2008)[c]
Kd_V	0.175	(Mayer et al., 1984)[a,c]
α	0.15	(Mayer et al., 1984)[c]
n_V	6	(Mayer et al., 1984)[c]
τ_{CaN}	3000 ms	(Quintana et al., 2005)
τ_{PKA}	2000 ms	(Urakubo et al., 2008)[c]
τ_{CaMKII}	8000 ms	(Urakubo et al., 2008)[c]
τ_{PP1}	8000 ms	
Kd_{CaN}	0.02	(Urakubo et al., 2008)[a,c]
n_{CaN}	10	(Urakubo et al., 2008)[c]
Kd_{PKA}	0.08	(Urakubo et al., 2008)[a,c]
n_{PKA}	5	(Urakubo et al., 2008)[c]
Kd_{CaMKII}	0.21	(Urakubo et al., 2008)[a,c]
n_{CaMKII}	30	(Urakubo et al., 2008; Zhabotinsky, 2000)[c]
Kd_{PP1}	0.7	(Urakubo et al., 2008)[a,c]
n_{PP1}	2	(Urakubo et al., 2008)[c]
Amp_{LTP}	70%	(Urakubo et al., 2008)[a,c]
Amp_{LTD}	70%	(Urakubo et al., 2008)[a,c]

[a] Molecular concentrations, dissociation constants, and amplification factors are dimensionless.
[b] τ_{NMDAR} and τ_{BAP} are the time constants of alpha functions that includes both activation and inactivation time constants of NMDARs and BAP, respectively (see (A.4), (C.1) and (C.4) in Appendix).
[c] The parameters were estimated according to reproduce the behavior in the detailed model (Urakubo et al., 2008). Note that parameters in the reduced model do not directly correspond to those in experiments nor to biophysical parameters in the detailed model because parameters in the reduced model can be regarded as compressed parameters of several reactions.

According to the system model, the essential framework of signal processing in the induction of cerebellar LTD is comprised of one upstream and one downstream subsystem (Fig. 2(B)). The

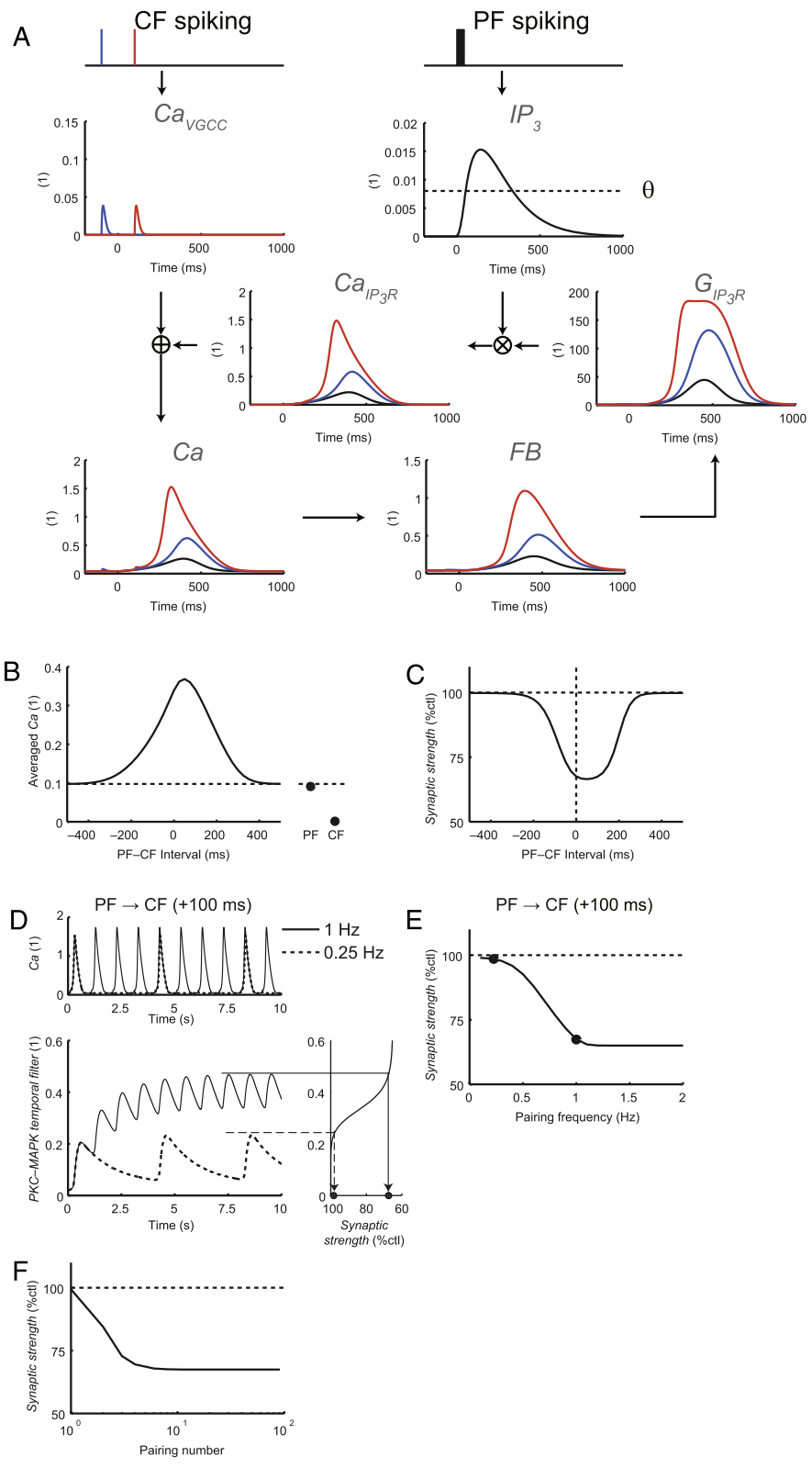

Fig. 3. Signal processing in the induction of cerebellar LTD. (A) The sample time profiles of *Ca* and IP_3 signals in the IP_3R subsystem. Red lines show the burst PF spiking preceded the CF spiking by 100 ms (T_{CF}–$T_{PF} = +100$ ms), blue lines show the burst PF spiking followed the CF spiking by 100 ms (T_{CF}–$T_{PF} = -100$ ms), and black lines show PF spiking alone. θ represents the transition threshold of Ca_{IP_3R} signals (see Supplemental Fig. 1(B)). (B, C) Time window of the averaged *Ca* (time integration of *Ca* signals) (B) and synaptic strength (C) induced by pairing frequency with 1 Hz for 60 s in the system model. (D) The responses of the PKC–MAPK subsystem to repetitive pairing of PF and CF spiking (T_{PF}–$T_{CF} = +100$ ms) at 1 Hz for 60 s (solid line) and at 0.25 Hz for 60 s (dashed line). The peak amplitude of signals from the PKC–MAPK temporal filter was transformed through switch-like nonlinear functions to synaptic strength. (E) The pairing-frequency-dependent changes of synaptic strength (T_{PF}–$T_{CF} = +100$ ms). (F) The pairing-numbers-dependent changes of synaptic strength (T_{PF}–$T_{CF} = +100$ ms at 1 Hz).

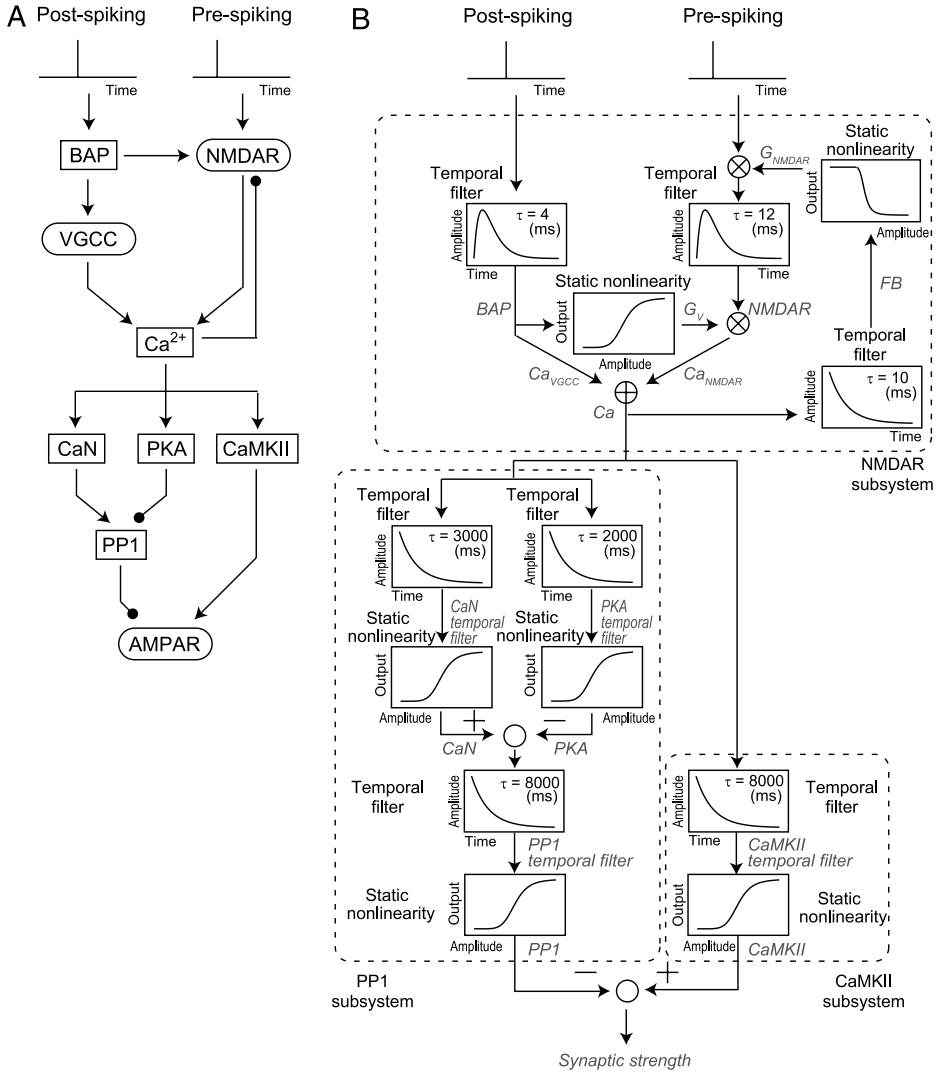

Fig. 4. The kinetic and system models of cortical STDP. Input signals (pre-spiking and post-spiking) were converted to the changes of synaptic strength. (A) The kinetic model of cortical STDP. The squares enclose names of intracellular molecules, and the rounded squares enclose names of channels or receptors. The arrows depict the relations between upstream and downstream. The sharp arrowhead activation, and the circles indicate suppression. (B) The system model of cortical STDP, which consists of temporal filters and static nonlinear functions. The arrows depict the information flows. Gray and italic words indicate names of signals (variables). Curves in the square boxes depict shapes of the filters and functions. τ represents the time constant of each filter. The dashed boxes enclose the feedback subsystems and downstream subsystems.

upstream subsystem is denoted as the inositol 1,4,5-trisphosphate receptor (IP_3R) subsystem. In this subsystem, PF spiking led to the generation of IP_3 (IP_3) and IP_3-mediated Ca^{2+} signal (Ca_{IP_3R}), and CF spiking led to a VGCC-mediated Ca^{2+} signal (Ca_{VGCC}). Only when PF spiking was followed by CF spiking in the time window from −200 to 300 ms (Fig. 3(B)), the pairing of PF and CF spiking 'induced' the regenerative cycle of Ca^{2+}, which was described by a feedback filter and a bell-shaped nonlinear function in the system model. The output signal from the IP_3R subsystem (Ca) was transformed by the temporal filter (FB) and bell-shaped nonlinear function (G_{IP_3R}), and the filtered signal (G_{IP_3R}) was used for multiplication by the signal from PF spiking, IP_3 (Figs. 2(B) and 3(A)). Because the nonlinear function for G_{IP_3R} has a bell shape (Bezprozvanny, Watras, & Ehrlich, 1991), the IP_3R subsystem acts as positive feedback at a lower signal level and negative feedback at a higher signal level. Thus, the signal from the IP_3R subsystem is transient. The time window of the regenerative cycle of Ca^{2+} was determined by the temporal filter of PF spiking (Fig. 3(B), Supplemental Fig. 1) and consequently LTD (Fig. 3(C)). Thus, the multiplication of signals from the IP_3R feedback subsystem and the temporal filter of PF spiking is the mechanism underlying the detection of the timing between PF and CF spiking.

Ca^{2+} was then transferred to the downstream protein kinase C (PKC)—mitogen activated-protein kinase (MAPK) subsystem with temporal filters (*PKC–MAPK temporal filter*) and static nonlinear functions (*Synaptic strength*). We used the PKC–MAPK subsystem, which has been determined as the leaky integrate-and-fire mechanism proposed by Tanaka et al. (2007). The time constant of the temporal filter of the PKC–MAPK subsystem (1520 ms) was much larger than those of the upstream subsystem (80 ms) and the temporal filter of PF spiking (120 ms). Therefore, the integration of signals in the PKC–MAPK subsystem requires the pairing interval of PF and CF spiking to be shorter than 1520 ms (Fig. 3(D), *PKC–MAPK temporal filter*), and a pairing frequency of less than 1 Hz did not induce LTD. (Fig. 3(E)). Spontaneous and maximal CF-spiking rates have been shown to be about 1 Hz and a few hertz (Welsh, 2002), respectively, suggesting that the CF spiking is likely to limit the pairing-frequency *in vivo*. Considering this fact, the PKC–MAPK subsystem can integrate signals of PF and CF spiking *in vivo*. Thus, the time constant of the temporal filter in the PKC–MAPK subsystem determines the pairing frequency necessary for LTD induction. The integrated signal was transformed in a switch-like manner by the static nonlinear function, which corresponds to a PKC–MAPK positive

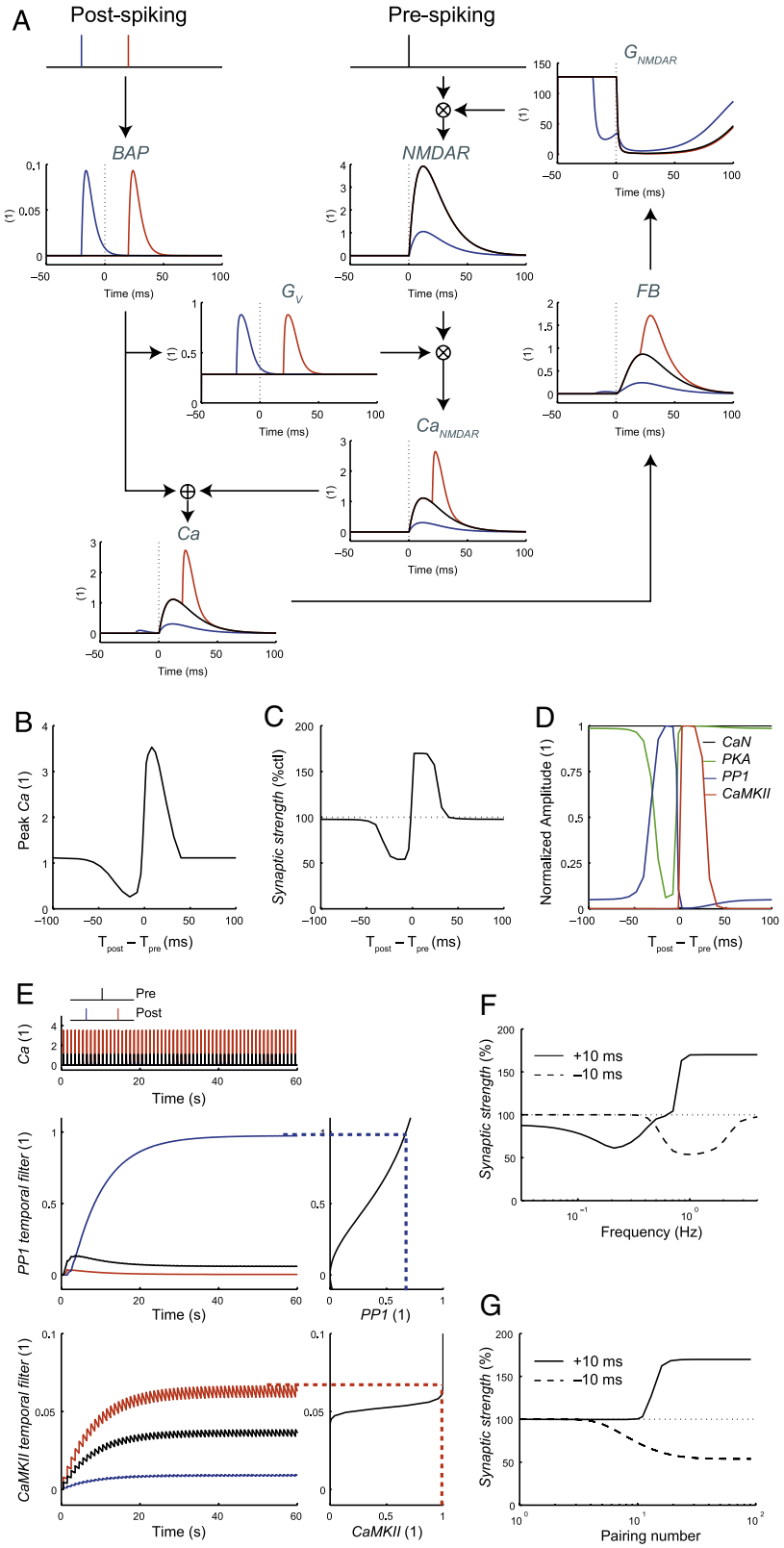

Fig. 5. Signal processing in the induction of cortical STDP. (A) The sample time profiles of *Ca* and G_{NMDAR} signals in the NMDAR subsystem. Red lines indicate positive timing with 20 ms interval ($T_{post}-T_{pre} = +20$ ms), blue lines indicate the negative timing with 20 ms interval ($T_{post}-T_{pre} = -20$ ms), and black lines indicate pre-spiking alone. (B–D) The time window of the peak *Ca* amplitude in the system model (B), synaptic strength induced by the pairing frequency with 1 Hz for 60 s (C), and the normalized peak amplitudes of *CaN* signals (black line), *PKA* signals (green line), *PP*1 signals (blue line), and *CaMKII* signals (red line) (D) in the system model of cortical STDP. (E) The responses of *PP*1 and *CaMKII* signals to repetitive pairing of pre- and post-spiking at 1 Hz for 60 s. Red lines indicate the positive timing with 10 ms interval, blue lines indicate the negative timing with 10 ms interval, and black lines indicate pre-spiking alone. The peak amplitude of *PP*1 and *CaMKII* signals were transformed through switch-like nonlinear functions and summed into synaptic strength, leading to LTD and LTP, respectively. (F) The pairing-frequency-dependent changes of synaptic strength in the positive timing with 10 ms interval (solid line) and in the negative timing with 10 ms interval (dashed line). (G) The pairing-numbers-dependent changes of synaptic strength in the positive timing with 10 ms interval (solid line) and in the negative timing with 10 ms interval (dashed line), both of which were given at 1 Hz.

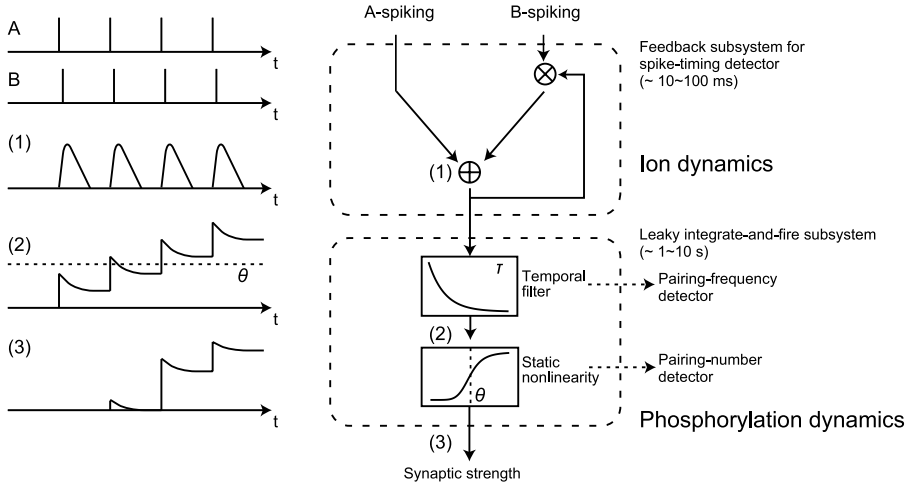

Fig. 6. Common framework of signal processing in synaptic plasticity. The signal processing of both cerebellar LTD and cortical STDP consist conceptually of upstream and downstream subsystems. The upstream subsystem uses multiplication of signals from the feedback filters with shorter time constant (∼10–100 ms) and nonlinear functions, and it detects spike-timing information (1). The downstream subsystem consists of the temporal filter with a longer time constant (∼1–10 s) and a switch-like static nonlinear function, which serves as a leaky integrate-and-fire system. The temporal filter with a longer time constant determines pairing frequency (2), and the switch-like static nonlinear function determines pairing numbers (3) when pairing frequency is much faster than the time constant of the temporal filter necessary to induce change of synaptic strength.

feedback loop (Bhalla & Iyengar, 1999; Kuroda et al., 2001; Tanaka & Augustine, 2008; Tsuruno & Hirano, 2007). When the pairing interval of PF and CF spiking was faster than the time constant of the temporal filter, the repetitive signals were integrated, and when the integrated signal exceeded the threshold of the static nonlinear function, synaptic strength changed (Fig. 3(D) and (F), *Synaptic strength*). This means that the threshold of the static nonlinear function can determine the pairing numbers necessary for LTD induction (Fig. 3(F)), because a lower threshold requires fewer pairing numbers and a higher threshold requires more. Thus, the downstream PKC–MAPK subsystem determines the pairing frequency and pairing numbers required for cerebellar LTD.

In summary, the upstream IP_3R subsystem detects the timing between PF and CF spiking by using feedback multiplication, and the downstream PKC–MAPK subsystem detects the pairing frequency and pairing numbers of PF and CF spiking required for the induction of LTD by using the leaky integrate-and-fire system. This is the essential framework of signal processing in the induction of cerebellar LTD.

2.3. System model of cortical STDP

By using temporal filters and static nonlinear functions, we also developed a system model of cortical STDP, which consists of 16 variables to describe the representative signaling activities (Fig. 4, gray and italic words; Appendix C). Repetitive pairing of a pre-spike followed by a post-spike, denoted as positive timing, induced larger Ca^{2+} (*Ca*), and consequently increased synaptic strength (i.e., LTP), whereas repetitive pairing of a post-spike followed by a pre-spike, denoted as negative timing, induced smaller *Ca* and decreased synaptic strength (i.e., LTD; Fig. 5(A)–(C)) (Froemke, Poo, & Dan, 2005; Koester & Sakmann, 1998; Lisman, 2001; Urakubo et al., 2008).

The system model of cortical STDP revealed the essential framework of signal processing in the induction of cortical STDP, with one upstream and two downstream subsystems (Fig. 4(B)). Timing between pre- and post-spiking was detected by two types of multiplication of pre-spiking by a backpropagating action potential (BAP) from post-spiking (*BAP*) and by a feedback signal from the output *Ca* signal (G_{NMDAR}) in the *N*-methyl *D*-aspartate receptor (NMDAR) subsystem (Fig. 4(B)). In pairing, pre-spiking activated NMDARs (*NMDAR*) and post-spiking initiated a BAP (*BAP*), respectively. In the positive timing, multiplication of NMDAR and *Gv* induced larger Ca_{NMDAR} (Fig. 5(A), red line), where *Gv* corresponds to release of Mg^{2+}-block of NMDARs by a BAP (*BAP*) in the kinetic model. This multiplication of NMDAR and *Gv* is a feedforward multiplication. The time window of LTP was determined by the temporal filter of pre-spiking (Supplemental Fig. 2(B)). In contrast, in the negative-timing, the signal induced by post-spiking was transferred to a feedback filter (*FB*) and a nonlinear function (G_{NMDAR}) in the NMDAR subsystem. Because the output signal from this nonlinear function decreased as the input signal to this function increased, the output signal from this subsystem (G_{NMDAR}) became smaller as the signal from post-spiking became larger. Thus, this subsystem acts as a negative feedback. G_{NMDAR} was then multiplied by the signal of pre-spiking, resulting in reduction of NMDAR and consequently of Ca_{NMDAR} in the negative-timing (Fig. 5(A), blue line), which corresponds to the allosteric inhibition of NMDARs in the kinetic model (Urakubo et al., 2008). The time window of LTD was determined by the temporal filter of the negative feedback (Supplemental Fig. 2(A)). Thus, the positive-timing was detected by feedforward multiplication of NMDAR and *Gv*, and the negative-timing was detected by feedback multiplication of a post-spiking signal through the feedback filter and the nonlinear decreasing function (G_{NMDAR}) and pre-spiking.

Ca^{2+} was then transferred to two downstream subsystems: the protein phosphatase 1 (PP1) and Ca^{2+}/calmodulin dependent protein kinase II (CaMKII) subsystems. The PP1 and CaMKII subsystems serve as selective decoders of lower and higher Ca^{2+} signals (*Ca*), respectively, through different Ca^{2+} sensitivity of the static nonlinear functions (Fig. 5(D), Supplemental Fig. 3). The signal of lower *Ca* selectively induced a PP1 signal (*PP1*) through the balance of signals between calcineurin (*CaN*) and protein kinase A (*PKA*) through high and middle Ca^{2+} sensitivity of the static nonlinear functions, respectively, which negatively regulate synaptic strength (Fig. 5(E), Supplemental Fig. 4). This means that the PP1 subsystem is a decoder of the negative-timing information into LTD. The signal of higher Ca^{2+} selectively induced a CaMKII signal (*CaMKII*) through low Ca^{2+} sensitivity of the static nonlinear function (Fig. 5(D), Supplemental Fig. 3), which positively regulates synaptic strength. This means that the CaMKII subsystem is a decoder of the positive-timing information into LTP. The time constants of both subsystems (8 s) were larger than those of the

NMDAR subsystem, and therefore integration of the signals at the PP1 and CaMKII subsystems requires the pairing interval of pre- and post-spiking to be shorter than 8 s (Fig. 5(E)). Consistent with this, a pairing frequency of pre- and post-spiking of 0.2 Hz ($1/5\ s^{-1}$) has been shown to induce STDP in some pyramidal neurons (Froemke & Dan, 2002). Because of the large time constants of the PP1 and CaMKII subsystems, the subsystems can integrate the signal with such a low pairing frequency. Thus, the time constants of the PP1 and CaMKII subsystem determine the pairing-frequency required for the induction of cortical STDP. The integrated signals of CaMKII and PP1 were transformed in a switch-like manner by the static nonlinear functions, corresponding to a CaMKII positive feedback loop (Dupont, Houart, & De Koninck, 2003; Okamoto & Ichikawa, 2000; Urakubo et al., 2008; Zhabotinsky, 2000) and cooperative CaN activation (Feng & Stemmer, 2001; Stemmer & Klee, 1994), respectively. When the pairing intervals in the positive and negative timing were faster than the time constant of the CaMKII and PP1 subsystems, the signals were integrated and reached the threshold, leading to LTP and LTD, respectively (Fig. 5(F), *Synaptic strength*). This means that the thresholds of the static nonlinear functions of the CaMKII and PP1 subsystems can determine the pairing-numbers necessary for LTP and LTD induction (Fig. 5(G)), because the lower thresholds of the static nonlinearity of PP1 and CaMKII require fewer pairing numbers for LTD and LTP, respectively, and their higher thresholds require more. This is consistent with the experimental observation that the pairing-numbers required for both LTD and LTP were around 60 times in cortical STDP (Froemke, Tsay, Raad, Long, & Dan, 2006). Thus, the downstream subsystems can determine the pairing-frequency and pairing-numbers required for cortical STDP.

In summary, the NMDAR subsystem detects the timing between pre- and post-spiking by use of feedforward and feedback multiplications, and the CaMKII and PP1 subsystems detect lower and higher Ca^{2+} signals, respectively, and determine the pairing-frequency and pairing-numbers required for induction of LTP and LTD, respectively by use of parallel leaky integrate-and-fire systems. This is the essential framework of signal processing in the induction of cortical STDP.

3. Discussion

A common framework achieves the induction of both cerebellar LTD and cortical STDP (Fig. 6). Both systems have upstream subsystems for spike-timing detection, namely the IP_3R subsystem in cerebellar LTD and the NMDAR subsystem in cortical STDP. Both subsystems use feedback multiplication of signals from the feedback filters and nonlinear functions as well as from inputs for the spike-timing detection for LTD. The NMDAR subsystem uses feedforward multiplication of pre- and post-spiking signals for spike-timing detection for LTP. Both subsystems mainly use ion dynamics, and the scale of the time constants of both upstream subsystems are in the range of about 10–100 ms, which were obtained by those in the biophysical and biochemical models (Doi et al., 2005; Naoki, Sakumura, & Ishii, 2005; Urakubo et al., 2008) and in experiments (Bezprozvanny et al., 1991; Lester, Clements, Westbrook, & Jahr, 1990; Nevian & Sakmann, 2004; Sabatini, Oertner, & Svoboda, 2002; Wang et al., 2000). The two frameworks of signal processing have common characteristics of spike-timing detection in both subsystems.

In addition, both systems have downstream subsystems for pairing-frequency and pairing-numbers detection, namely the PKC–MAPK subsystem in cerebellar LTD and the CaMKII and PP1 subsystems in cortical STDP. Both subsystems mainly use phosphorylation dynamics and a temporal filter with longer time constants (∼1–10 s) followed by nonlinear switch-like functions, which serve as leaky integrate-and-fire systems of upstream signals. The time constants of the temporal filters in the downstream subsystem determine the pairing frequency necessary for the induction of synaptic plasticity. The time constants of the downstream subsystems were obtained from the biophysical and biochemical models (Bhalla & Iyengar, 1999; Kuroda et al., 2001; Ogasawara, Doi, Doya, & Kawato, 2007; Urakubo et al., 2008) and in experiments (De Koninck & Schulman, 1998; Tanaka et al., 2007). The switch-like responses of the static nonlinearity functions determine the pairing numbers necessary for the induction of synaptic plasticity. The higher the threshold becomes, the more pairing numbers are required. The two frameworks of signal processing have common characteristics of pairing-frequency and pairing-numbers detection in both subsystems. Here we focused on the early phase of long-term synaptic plasticity. The late-phase of synaptic plasticity has been shown to involve gene and protein expression, which presumably has longer time scales on the order of minutes and hours.

In the system models, we reduced the detailed kinetic models of cerebellar LTD and cortical STDP to capture the essential characteristics, rather than to make the most effectively reduced model. For effective model reduction, many mathematical methods have been proposed (e.g. Okino & Mavrovouniotis, 1998). Based on the methods, a target model will be simplest, but may be unintuitive in some cases. The system modeling approach is beneficial to explain synaptic plasticity on the basis of signaling pathways sufficiently simply and more intuitively.

In conclusion, our system models highlight the common frameworks underlying the induction of both types of synaptic plasticity, regardless of the fact that different molecules and networks are involved in the induction of cerebellar LTD and cortical STDP.

Acknowledgments

We thank K. Tanaka-Yamamoto for critical reading of the manuscript and members of our laboratory for helpful comments. This work was supported by the National Project "Next Generation Integrated Living Matter Simulation", and Grant-in-Aid for Young Scientists (B) (#23700371) of the Ministry of Education, Culture, Sports, Science, and Technology of Japan (MEXT), and a grant from the Core Research for Evolutional Science and Technology (CREST), Japan Science and Technology (JST). M.H. was a research fellow of the Japan Society for the Promotion of Science.

Appendix A. Temporal filter and static nonlinear functions of the systems models

We reduced the detailed kinetic models of cerebellar LTD and cortical STDP (Fig. 1) by employing two types of linear temporal filters and static nonlinear functions (Endeman & Kamermans, 2010). The two types of the linear temporal filters are defined by

$$Output(t) = \int_{-\infty}^{t} dt' \cdot Input(t') \cdot f_{TF1}(t - t'; \tau), \tag{A.1}$$

$$f_{TF1}(t; \tau_X) = \begin{cases} \dfrac{1}{\tau_X} \exp\left(-\dfrac{t}{\tau_X}\right), & (0 \le t) \\ 0, & \text{otherwise}, \end{cases} \tag{A.2}$$

$$Output(t) = \int_{-\infty}^{t} dt' \cdot Input(t') \cdot f_{TF2}(t - t'; \tau), \tag{A.3}$$

$$f_{TF2}(t; \tau_X) = \begin{cases} \dfrac{t}{\tau_X^2} \exp\left(-\dfrac{t}{\tau_X}\right), & (0 \le t) \\ 0, & \text{otherwise}, \end{cases} \tag{A.4}$$

where t is the time, X is the index of the filter, τ_x is the time constant, and $f_{TF1}(t; \tau)$ and $f_{TF2}(t; \tau)$ is the kernel functions.

The static nonlinear function is described by the following Hill equation:

$$Output(t) = g_{Hill}\left[Input(t); Kd_X, n_X\right], \tag{A.5}$$

$$g_{Hill}(Input; Kd_X, n_X) = \frac{Input^{n_X}}{Kd_X^{n_X} + Input^{n_X}}, \tag{A.6}$$

where $Input(t)$ is the input, Kd_x is the dissociation constant, n_x is the Hill coefficient, and $g_{Hill}[Input(t); Kd_X, n_x]$ is the Hill equation. This Hill equation is used, except that the bell-shaped function is also used as a nonlinear filter in Eq. (B.3).

Appendix B. Cerebellar LTD model

Using the linear temporal filters and static nonlinear functions, we developed a system model of cerebellar LTD (Fig. 2, Table 1). The model had one upstream and one downstream subsystem, denoted as the IP_3R and the PKC–MAPK subsystems, respectively. The construction of these subsystems is described in the following sections.

IP_3R subsystem

PF-spiking leads to the generation of IP_3. The dynamics of IP_3, $IP_3(t)$, is described as follows:

$$IP_3(t) = \int_{-\infty}^{t} dt' \cdot \sum_i \delta(t_{PF}^i - t') \cdot f_{TF2}(t - t'; \tau_{PF}), \tag{B.1}$$

where $\delta(t)$ is the Dirac's delta function, which converts PF-spiking events to unit impulses in time; t_{PF}^i is the time of the ith PF-spiking event; and τ_{PF} is the time constant of IP_3 generation. IP_3-induced Ca^{2+} release, Ca_{IP_3R}, is described by

$$Ca_{IP_3R}(t) = G_{IP_3R}(t) \cdot IP_3(t), \tag{B.2}$$

where G_{IP_3R} is the Ca^{2+}-dependent component of IP_3R. G_{IP_3R} is described by

$$G_{IP_3R}(t) = Amp_{IP_3R} \cdot \left\{ \frac{k \cdot FB(t)}{[k + FB(t)] \cdot [K + FB(t)]} \right\}^{n_{IP_3R}}, \tag{B.3}$$

$$FB(t) = \int_{-\infty}^{t} dt' \cdot Ca(t') \cdot f_{TF1}(t - t'; \tau_{FB}), \tag{B.4}$$

where Amp_{IP_3R}, k, K, and n_{IP_3R} are the gain, lower, and higher sensitivity constants and the order of the IP_3R bell-shape function, respectively; $Ca(t)$ is the total Ca^{2+} increase as described below; and τ_{FB} is the time constant of Ca^{2+} feedback.

In turn, CF spiking leads to a VGCC-mediated Ca^{2+} signal, Ca_{VGCC}, as follows:

$$Ca_{VGCC}(t) = \int_{-\infty}^{t} dt' \cdot \sum_i \delta(t_{CF}^i - t') \cdot f_{TF2}(t - t'; \tau_{CF}), \tag{B.5}$$

where $\delta(t)$ is the Dirac's delta function, t_{CF}^i is the time of the ith CF-spiking event, and τ_{CF} is the time constant of the Ca^{2+} signal. Together with Ca_{IP_3R}, the total Ca^{2+} signal, Ca, is

$$Ca(t) = Ca_{basal} + Ca_{VGCC}(t) + Ca_{IP_3R}(t), \tag{B.6}$$

where Ca_{basal} is the basal Ca^{2+} signal. The basal Ca^{2+} signal was required for the regenerative cycle of Ca^{2+} triggered just by a PF-spike burst followed by a CF spike. In the IP_3R subsystem, $Ca(t)$ is normalized as integrated $Ca_{VGCC}(t)$ by a single CF spike becomes 1.

PKC–MAPK subsystem

In the PKC–MAPK subsystem, Ca filtered through the temporal filter, *PKC–MAPK temporal filter* (t), and through static nonlinearity, *LTD*, and the final readout, *Synaptic strength*, are defined by

$$\text{PKC–MAPK temporal filter}(t) = \int_{-\infty}^{t} dt' \cdot Ca(t') \cdot f_{TF1}(t - t'; \tau_{ST}), \tag{B.7}$$

$$LTD = Amp_{ST} \cdot \max_t \{g_{Hill}[\text{PKC–MAPK temporal filter}(t); Kd_{ST}, n_{ST}]\}, \tag{B.8}$$

$$Synaptic\ strength = 100 - LTD, \tag{B.9}$$

where τ_{ST} is the time constant of the low-pass filter in the PKC–MAPK subsystem, and Amp_{ST}, Kd_{ST}, and n_{ST} are the gain and dissociation constants and the Hill coefficient of the nonlinear function in the PKC–MAPK subsystem, respectively.

Appendix C. Cortical STDP model

Using the linear temporal filters and static nonlinear functions, we developed a system model of cortical STDP (Fig. 4, Table 2), which consisted of one upstream subsystem (NMDAR) and two downstream subsystems (PP1 and CaMKII). The construction of these subsystems is described in the following sections.

NMDAR subsystem

Pre-spiking leads to the activation of NMDARs, NMDAR, as follows:

$$NMDAR(t) = \int_{-\infty}^{t} dt' \cdot \sum_i G_{NMDAR}(t_{pre}^i) \cdot \delta(t_{pre}^i - t') \cdot f_{TF2}(t - t'; \tau_{NMDAR}), \tag{C.1}$$

where $\delta(t)$ is the Dirac's delta function, t_{pre}^i is the time of ith pre-spiking event, τ_{NMDAR} is the time constant of NMDAR activation, and G_{pre} is the negative regulatory component from a feedback filter. G_{pre} is defined as:

$$G_{NMDAR}(t) = \frac{Amp_{NMDAR}}{\kappa^{n_{FB}} + FB(t)^{n_{FB}}}, \tag{C.2}$$

$$FB(t) = \int_{-\infty}^{t} dt' \cdot Ca(t') \cdot f_{TF1}(t - t'; \tau_{FB}), \tag{C.3}$$

where κ and n_{FB} are the dissociation constant and Hill coefficient of the static nonlinear function, respectively; τ_{FB} is the time constant of the temporal filter of the allosteric feedback inhibition of NMDARs; and $Ca(t)$ is the total Ca^{2+} signal.

In turn, post-spiking leads to a BAP, $BAP(t)$. BAP negatively regulates a Ca^{2+} signal via NMDARs, $Ca_{NMDAR}(t)$, and leads to a Ca^{2+} signal via VGCC, $Ca_{VGCC}(t)$. $BAP(t)$, $G_V(t)$, $Ca_{NMDAR}(t)$, and $Ca_{VGCC}(t)$ are defined as:

$$BAP(t) = \int_{-\infty}^{t} dt' \cdot \sum_i \delta(t_{post}^i - t') \cdot f_{TF2}(t - t'; \tau_{BAP}), \tag{C.4}$$

$$G_V(t) = \frac{[BAP(t) + \alpha]^{n_V}}{Kd_V^{n_V} + [BAP(t) + \alpha]^{n_V}} \tag{C.5}$$

$$Ca_{NMDAR}(t) = G_V \cdot NMDAR(t), \tag{C.6}$$

$$Ca_{VGCC}(t) = BAP(t), \tag{C.7}$$

where t_{post}^i is the time of ith post-spiking event, and τ_{BAP}, n_V, Kd_V, and α are the time constant, Hill coefficient, dissociation constant, and resting potential of BAP, respectively. Together, the total Ca^{2+} signal, $Ca(t)$, is

$$Ca(t) = Ca_{VGCC}(t) + Ca_{NMDAR}(t). \tag{C.8}$$

In the NMDAR subsystem, $Ca(t)$ is normalized as integrated $Ca_{VGCC}(t)$ by a single post-spike becomes 1.

*PP*1 *subsystem*

In the PP1 subsystem, based on *Ca*, the activation of CaN (*CaN*), PKA (*PKA*), and PP1 (PP1) are calculated by

$$\text{CaN temporal filter}(t) = \int_{-\infty}^{t} dt' \cdot Ca(t') \cdot f_{TF1}(t - t'; \tau_{CaN}), \quad \text{(C.9)}$$

$$CaN(t) = g_{Hill}\left[\text{CaN temporal filter}(t), Kd_{CaN}, n_{CaN}\right], \quad \text{(C.10)}$$

$$\text{PKA temporal filter}(t) = \int_{-\infty}^{t} dt' \cdot Ca(t') \cdot f_{TF1}(t - t'; \tau_{PKA}), \quad \text{(C.11)}$$

$$PKA(t) = g_{Hill}\left[\text{PKA temporal filter}(t), Kd_{PKA}, n_{PKA}\right], \quad \text{(C.12)}$$

$$\text{PP1 temporal filter}(t) = \int_{-\infty}^{t} \cdot[CaN(t') - PKA(t')] \cdot f_{TF1}(t - t'; \tau_{PP1})dt', \quad \text{(C.13)}$$

$$PP1(t) = g_{Hill}\left[\text{PP1 temporal filter}(t), Kd_{PP1}, n_{PP1}\right], \quad \text{(C.14)}$$

where $\{\tau_{CaN}, Kd_{CaN}, n_{CaN}\}$, $\{\tau_{PKA}, Kd_{PKA}, n_{PKA}\}$, and $\{\tau_{PP1}, Kd_{PP1}, n_{PP1}\}$ are the {time constant, dissociation constant, Hill coefficient} of CaN, PKA, and PP1, respectively.

CaMKII subsystem

In the CaMKII subsystem, the activation of CaMKII (*CaMKII*) is calculated by

$$\text{CaMKII temporal filter}(t) = \int_{-\infty}^{t} dt' \cdot Ca(t') \cdot f_{TF1}(t - t'; \tau_{CaMKII}), \quad \text{(C.15)}$$

$$CaMKII(t) = g_{Hill}[\text{CaMKII temporal filter}(t), Kd_{CaMKII}, n_{CaMKII}], \quad \text{(C.16)}$$

where τ_{CaMKII}, Kd_{CaMKII}, and n_{CaMKII} are the time constant, dissociation constant, and Hill coefficient of CaMKII, respectively. Based on $PP1(t)$ and $CaMKII(t)$, the final readout, *Synaptic strength*, is defined by

$$LTP = Amp_{LTP} \cdot \max_t\left[CaMKII(t)\right], \quad \text{(C.17)}$$

$$LTD = Amp_{LTD} \cdot \max_t\left[PP1(t)\right], \quad \text{(C.18)}$$

$$\textit{Synaptic strength} = 100 + LTP\text{–}LTD. \quad \text{(C.19)}$$

Appendix D. Numerical simulation

The software Matlab (Mathworks Inc., Natick, MA, USA) was used for simulation and analyses. Sample programs are available for download at http://www.kurodalab.org/info/SystemModel/index.html. For efficient computation, the algorithm of the ARMA filter was used. For the computation of the cerebellar LTD model, a 1 ms time step was used. For the computation of the cortical STDP model, a 0.1 ms time step was used.

Appendix E. Supplementary data

Supplementary material related to this article can be found online at http://dx.doi.org/10.1016/j.neunet.2013.01.018.

References

Alon, U. (2007). Network motifs: theory and experimental approaches. *Nature Reviews Genetics*, *8*, 450–461.

Bezprozvanny, I., Watras, J., & Ehrlich, B. E. (1991). Bell-shaped calcium-response curves of Ins(1,4,5)P_3- and calcium-gated channels from endoplasmic reticulum of cerebellum. *Nature*, *351*, 751–754.

Bhalla, U. S., & Iyengar, R. (1999). Emergent properties of networks of biological signaling pathways. *Science*, *283*, 381–387.

Brown, S. A., Morgan, F., Watras, J., & Loew, L. M. (2008). Analysis of phosphatidylinositol-4,5-bisphosphate signaling in cerebellar Purkinje spines. *Biophysical Journal*, *95*, 1795–1812.

Caporale, N., & Dan, Y. (2008). Spike timing-dependent plasticity: a Hebbian learning rule. *Annual Review of Neuroscience*, *31*, 25–46.

De Koninck, P., & Schulman, H. (1998). Sensitivity of CaM kinase II to the frequency of Ca^{2+} oscillations. *Science*, *279*, 227–230.

Doi, T., Kuroda, S., Michikawa, T., & Kawato, M. (2005). Inositol 1,4,5-trisphosphate-dependent Ca^{2+} threshold dynamics detect spike timing in cerebellar Purkinje cells. *Journal of Neuroscience*, *25*, 950–961.

Doya, K. (2000). Complementary roles of basal ganglia and cerebellum in learning and motor control. *Current Opinion in Neurobiology*, *10*, 732–739.

Dupont, G., Houart, G., & De Koninck, P. (2003). Sensitivity of CaM kinase II to the frequency of Ca^{2+} oscillations: a simple model. *Cell Calcium*, *34*, 485–497.

Endeman, D., & Kamermans, M. (2010). Cones perform a non-linear transformation on natural stimuli. *Journal of Physiology*, *588*, 435–446.

Engert, F., Tao, H. W., Zhang, L. I., & Poo, M. M. (2002). Moving visual stimuli rapidly induce direction sensitivity of developing tectal neurons. *Nature*, *419*, 470–475.

Feldmeyer, D., Lubke, J., Silver, R. A., & Sakmann, B. (2002). Synaptic connections between layer 4 spiny neurone-layer 2/3 pyramidal cell pairs in juvenile rat barrel cortex: physiology and anatomy of interlaminar signalling within a cortical column. *Journal of Physiology*, *538*, 803–822.

Feng, B., & Stemmer, P. M. (2001). Ca^{2+} binding site 2 in calcineurin-B modulates calmodulin-dependent calcineurin phosphatase activity. *Biochemistry*, *40*, 8808–8814.

Froemke, R. C., & Dan, Y. (2002). Spike-timing-dependent synaptic modification induced by natural spike trains. *Nature*, *416*, 433–438.

Froemke, R. C., Poo, M. M., & Dan, Y. (2005). Spike-timing-dependent synaptic plasticity depends on dendritic location. *Nature*, *434*, 221–225.

Froemke, R. C., Tsay, I. A., Raad, M., Long, J. D., & Dan, Y. (2006). Contribution of individual spikes in burst-induced long-term synaptic modification. *Journal of Neurophysiology*, *95*, 1620–1629.

Hernjak, N., Slepchenko, B. M., Fernald, K., Fink, C. C., Fortin, D., Moraru, I. I., et al. (2005). Modeling and analysis of calcium signaling events leading to long-term depression in cerebellar Purkinje cells. *Biophysical Journal*, *89*, 3790–3806.

Honda, M., Urakubo, H., Tanaka, K., & Kuroda, S. (2011). Analysis of development of direction selectivity in retinotectum by a neural circuit model with spike timing-dependent plasticity. *Journal of Neuroscience*, *31*, 1516–1527.

Ito, M. (1989). Long-term depression. *Annual Review of Neuroscience*, *12*, 85–102.

Karmarkar, U. R., & Buonomano, D. V. (2002). A model of spike-timing dependent plasticity: one or two coincidence detectors?. *Journal of Neurophysiology*, *88*, 507–513.

Kawato, M. (1999). Internal models for motor control and trajectory planning. *Current Opinion in Neurobiology*, *9*, 718–727.

Kawato, M., Kuroda, S., & Schweighofer, N. (2011). Cerebellar supervised learning revisited: biophysical modeling and degrees-of-freedom control. *Current Opinion in Neurobiology*, *21*, 791–800.

Koester, H. J., & Sakmann, B. (1998). Calcium dynamics in single spines during coincident pre- and postsynaptic activity depend on relative timing of back-propagating action potentials and subthreshold excitatory postsynaptic potentials. *Proceedings of the National Academy of Sciences of the United States of America*, *95*, 9596–9601.

Kotaleski, J. H., Lester, D., & Blackwell, K. T. (2002). Subcellular interactions between parallel fibre and climbing fibre signals in Purkinje cells predict sensitivity of classical conditioning to interstimulus interval. *Integrative Physiological and Behavioral Science*, *37*, 265–292.

Kuroda, S., Schweighofer, N., & Kawato, M. (2001). Exploration of signal transduction pathways in cerebellar long-term depression by kinetic simulation. *Journal of Neuroscience*, *21*, 5693–5702.

Lester, R. A., Clements, J. D., Westbrook, G. L., & Jahr, C. E. (1990). Channel kinetics determine the time course of NMDA receptor-mediated synaptic currents. *Nature*, *346*, 565–567.

Linden, D. J., & Connor, J. A. (1995). Long-term synaptic depression. *Annual Review of Neuroscience*, *18*, 319–357.

Lisberger, S. G. (1998). Cerebellar LTD: a molecular mechanism of behavioral learning? *Cell*, *92*, 701–704.

Lisman, J. E. (2001). Three Ca^{2+} levels affect plasticity differently: the LTP zone, the LTD zone and no man's land. *Journal of Physiology*, *532*, 285.

Mayer, M. L., Westbrook, G. L., & Guthrie, P. B. (1984). Voltage-dependent block by Mg^{2+} of NMDA responses in spinal cord neurones. *Nature*, *309*, 261–263.

Naoki, H., Sakumura, Y., & Ishii, S. (2005). Local signaling with molecular diffusion as a decoder of Ca^{2+} signals in synaptic plasticity. *Molecular Systems Biology*, *1*, http://dx.doi.org/10.1038/msb4100035.

Nevian, T., & Sakmann, B. (2004). Single spine Ca^{2+} signals evoked by coincident EPSPs and backpropagating action potentials in spiny stellate cells of layer 4 in the juvenile rat somatosensory barrel cortex. *Journal of Neuroscience*, *24*, 1689–1699.

Ogasawara, H., Doi, T., Doya, K., & Kawato, M. (2007). Nitric oxide regulates input specificity of long-term depression and context dependence of cerebellar learning. *PLoS Computational Biology*, *3*, e179.

Okamoto, H., & Ichikawa, K. (2000). Switching characteristics of a model for biochemical-reaction networks describing autophosphorylation versus dephosphorylation of Ca^{2+}/calmodulin-dependent protein kinase II. *Biological Cybernetics*, *82*, 35–47.

Okino, M. S., & Mavrovouniotis, M. L. (1998). Simplification of mathematical models of chemical reaction systems. *Chemical Reviews*, *98*, 391–408.
Okubo, Y., Kakizawa, S., Hirose, K., & Iino, M. (2004). Cross talk between metabotropic and ionotropic glutamate receptor-mediated signaling in parallel fiber-induced inositol 1,4,5-trisphosphate production in cerebellar Purkinje cells. *Journal of Neuroscience*, *24*, 9513–9520.
Quintana, A. R., Wang, D., Forbes, J. E., & Waxham, M. N. (2005). Kinetics of calmodulin binding to calcineurin. *Biochemical and Biophysical Research Communications*, *334*, 674–680.
Rubin, J. E., Gerkin, R. C., Bi, G. Q., & Chow, C. C. (2005). Calcium time course as a signal for spike-timing-dependent plasticity. *Journal of Neurophysiology*, *93*, 2600–2613.
Sabatini, B. L., Oertner, T. G., & Svoboda, K. (2002). The life cycle of Ca^{2+} ions in dendritic spines. *Neuron*, *33*, 439–452.
Safo, P., & Regehr, W. G. (2008). Timing dependence of the induction of cerebellar LTD. *Neuropharmacology*, *54*, 213–218.
Schuett, S., Bonhoeffer, T., & Hubener, M. (2001). Pairing-induced changes of orientation maps in cat visual cortex. *Neuron*, *32*, 325–337.
Shouval, H. Z., Bear, M. F., & Cooper, L. N. (2002). A unified model of NMDA receptor-dependent bidirectional synaptic plasticity. *Proceedings of the National Academy of Sciences of the United States of America*, *99*, 10831–10836.
Sjostrom, P. J., Rancz, E. A., Roth, A., & Hausser, M. (2008). Dendritic excitability and synaptic plasticity. *Physiological Reviews*, *88*, 769–840.
Stemmer, P. M., & Klee, C. B. (1994). Dual calcium ion regulation of calcineurin by calmodulin and calcineurin B. *Biochemistry*, *33*, 6859–6866.
Tanaka, K., & Augustine, G. J. (2008). A positive feedback signal transduction loop determines timing of cerebellar long-term depression. *Neuron*, *59*, 608–620.
Tanaka, K., Khiroug, L., Santamaria, F., Doi, T., Ogasawara, H., Ellis-Davies, G. C., et al. (2007). Ca^{2+} requirements for cerebellar long-term synaptic depression: role for a postsynaptic leaky integrator. *Neuron*, *54*, 787–800.
Tsuruno, S., & Hirano, T. (2007). Persistent activation of protein kinase Calpha is not necessary for expression of cerebellar long-term depression. *Molecular and Cellular Neuroscience*, *35*, 38–48.
Tsuruno, S., & Hirano, T. (2011). Synaptic plasticity and motor learning in the cerebellum. In L. J. Pombano, & D. M. Evans (Eds.), *Cerebellum: anatomy, functions and disorders*. Nova Science Pub Inc.
Urakubo, H., Honda, M., Froemke, R. C., & Kuroda, S. (2008). Requirement of an allosteric kinetics of NMDA receptors for spike timing-dependent plasticity. *Journal of Neuroscience*, *28*, 3310–3323.
Urakubo, H., Honda, M., Tanaka, K., & Kuroda, S. (2009). Experimental and computational aspects of signaling mechanisms of spike-timing-dependent plasticity. *HFSP Journal*, *3*, 240–254.
Waltermann, C., & Klipp, E. (2011). Information theory based approaches to cellular signaling. *Biochimica et Biophysica Acta*, *1810*, 924–932.
Wang, S. S., Denk, W., & Hausser, M. (2000). Coincidence detection in single dendritic spines mediated by calcium release. *Nature Neuroscience*, *3*, 1266–1273.
Welsh, J. P. (2002). Functional significance of climbing-fiber synchrony: a population coding and behavioral analysis. *Annals of the New York Academy of Sciences*, *978*, 188–204.
Weng, G., Bhalla, U. S., & Iyengar, R. (1999). Complexity in biological signaling systems. *Science*, *284*, 92–96.
Yao, H., & Dan, Y. (2001). Stimulus timing-dependent plasticity in cortical processing of orientation. *Neuron*, *32*, 315–323.
Zhabotinsky, A. M. (2000). Bistability in the Ca^{2+}/calmodulin-dependent protein kinase-phosphatase system. *Biophysical Journal*, *79*, 2211–2221.